Document downloaded from:

http://hdl.handle.net/10251/183662

This paper must be cited as:

Magraner Benedicto, MT.; Montero Reguera, ÁE.; Cazorla-Marín, A.; Montagud- Montalvá, C.; Martos, J. (2021). Thermal response test analysis for U-pipe vertical borehole heat exchangers under groundwater flow conditions. Renewable Energy. 165:391-404. https://doi.org/10.1016/j.renene.2020.11.029

The final publication is available at

https://doi.org/10.1016/j.renene.2020.11.029

Copyright Elsevier

Additional Information

Thermal response test analysis for U-pipe vertical borehole heat exchangers under groundwater flow conditions

Teresa Magraner [a,*], Álvaro Montero [a], Antonio Cazorla-Marín [b], Carla Montagud-Montalvá [b], Julio Martos [c]

[a] *Departamento de Termodinámica Aplicada, Universitat Politècnica de València, Camino de Vera s/n, 46022 Valencia, Spain; almonter@upvnet.upv.es (A.M.)*

[b] *Instituto Universitario de Investigación de Ingeniería Energética (IUIIE), Universitat Politècnica de València, Camino de Vera s/n, 46022 Valencia, Spain; antonio.cazorla@iie.upv.es (A.C-M.), carmonmo@iie.upv.es (C, M-M.)*

[c] *Departamento de Ingeniería Electrónica, Universitat de València, Avda. de la Universitat s/n, 46100 Burjassot-Valencia, Spain; julio.martos@uv.es (J.M.)*

** Corresponding author: mmagbe@upv.es*

ABSTRACT

Conventional models used in the analysis of thermal response test data only consider conduction as heat transfer mechanism. In cases where presence of groundwater is detected, convection heat transmission plays an important role, so its influence must be determined in the calculation of the effective thermal conductivity, usually overestimated in these situations, increasing its value the higher the power injected and the time elapsed. In this work, based on the data collected in a borehole located at UPV (València) in which have been carried out three thermal response tests with different characteristics, has been implemented a variation of the finite line source model introducing an expression for the effective thermal conductivity formed by two terms, one static unaffected by underground flow and another dynamic that depends on time. Analyzing the data in the model developed and in the finite line source and infinite line source models, the results show that the new model estimates accurately the conductivity value unaffected by underground flow regardless the power injected or the time elapsed in the test, with differences between the results obtained in the analyzed tests and average thermal conductivity of 1,4%, compared to the conventional models in which this difference is 27%.

Keywords: Thermal response test (TRT) analysis; Geothermal heat exchanger; Ground water advection; Effective thermal conductivity; Borehole thermal resistance; Undisturbed ground temperature recovery

NOMENCLATURE

α	*ground thermal diffusivity*
C_v	*ground volumetric thermal capacity*
γ	*Euler constant*
Ei	*Euler integral*
λ	*effective ground thermal conductivity*
λ_0	*true ground thermal conductivity unaffected by groundwater flow*
L	*borehole depth*
$\dot{m}$	*fluid mass flow*
Q_z	*constant heat power injected to the ground per length unit*
R_b	*borehole thermal resistance*
r_b	*borehole radius*
$\mathrm{T_0}$	*undisturbed ground temperature*
$\mathrm{T_{in}}$	*fluid inlet temperature*
$\mathrm{T_{out}}$	*fluid outlet temperature*
T_{ave}	*average of the fluid temperature*
T_b	*temperature at the borehole surface*

1. INTRODUCTION

The most commonly used method to obtain the necessary data for ground source heat exchangers (GSHE) proper design in medium or large installations is the thermal response test (TRT), a procedure technically and economically accepted by designers [1-2] and promoters of shallow geothermal facilities, being used for more than two decades [3-4]. Thermal values obtained by following the indications described in regulations and standards [5-7] usually have no discussion among GSHE designers, regardless the limitation of the application of the model, the different ground characteristics and the measurements conditions in the work site. However, the measurement and analysis of the thermal ground parameters: ground thermal conductivity, borehole thermal resistance and undisturbed ground temperature [8-9] can be conditioned for different reasons. Actually, thermal conductivity measured in a thermal response test is called effective thermal conductivity because, due to the effects of an inhomogeneous ground and possible presence of groundwater flow, the heat transfer process is not pure conductive.

Thermal response test is carried out connecting a mobile equipment formed by a heating or cooling system, a hydraulic pump, flow and temperature sensors and a control system to a geothermal probe installed in a borehole in order to inject or extract a constant thermal power. Therefore, the first aspect to take into account in a TRT is the equipment control system, which must guarantee to perform the test under constant power conditions. For example, using a PID control system allows a more accurate analysis by reducing the error associated to the measurements [10]. Secondly, considering that the main outputs of the TRT are the inlet and outlet temperature of the heat carrier fluid as a function of time, minimizing the length of the connection pipes between the TRT equipment and the borehole should be a priority although sometimes it is not possible due to the work site conditions. In these cases, a filtering technique of the undesired effect produced in fluid temperature measurements by the ambient temperature can be used [11].

For data analysis and thermal parameters characterization different models are used [12], the most widely applied method is the infinite line source [13–17] but other approaches such as the finite line source model [18–21] or cylindrical source model [22–25] are also well known. These analytical models are used because of their simplicity and good accuracy of the results, mainly the infinite line source model, but a limitation to this methodology is the amount of groundwater flow [26]. As the effective ground thermal conductivity determined in TRT includes convection effects, in these cases its value is strongly conditioned. Advective phenomena, that is how groundwater flow transport the heat injected what depends on groundwater velocity, which is related to the hydrogeological characteristics of the different ground layers [27], are not being considering in the heat transfer models mentioned.

The effects of groundwater natural convection on borehole thermal resistance have been studied in groundwater-filled boreholes [28-29]. In grouted boreholes installed under groundwater flow conditions, the advective phenomena is relevant in borehole heat transfer boundary conditions. To consider it, several works proposed an analytical solution based on a moving finite line source model to consider the groundwater flow [30-33] introducing the Péclet dimensionless number in the heat transfer models. Other authors [34] have developed a new test protocol to evaluate the effects of convection and lateral groundwater flow based on the application of several heat injection and extraction pulses using a numerical model with a parameter estimation technique to obtain the thermal ground parameters. The incorporation of these proposals to the thermal response test analysis requires a computational effort, a longer period of data collection to minimize errors [35] or a reversible (heating and cooling) TRT equipment which supposes a barrier for the methodology standardization.

Although there are numerous methods to calculate the borehole thermal resistance [36] its estimation in situ by means of a TRT is important not only to obtain a value to carry out the shallow geothermal system dimensioning but also to verify the correct GSHE execution by comparing the measured with the expected value. Considering that the borehole resistance error is mainly influenced by the error of thermal conductivity [37], in ground source heat exchangers working under groundwater conditions, borehole resistance will also present the same positive effect than the effective thermal conductivity [38]. Performing several TRT varying the injection parameters [39–40] or enlarge the thermal response test duration [41] are adequate procedures to characterize properly the borehole thermal resistance. In this work, an accurate analysis of this parameter using three different heat injection ratios during long time periods is done.

Regarding the last ground thermal parameter that a TRT evaluates, undisturbed ground temperature, it is noted that this work is based on an exhaustive ground temperature characterization, measuring this value along the borehole depth before and during the thermal response test and evaluating the ground thermal recovery a long time after the end of the test, as is presented in previous works and collect in this contribution [42–43]. In this previous research, a standard analysis of thermal response test using infinite linear source model prediction can be found observing a deviation from the prediction of the infinite line model, showing an increase of the ground thermal conductivity with the advance of the test. To understand this phenomenon, the work developed in [44] presents an analysis procedure implemented by a 3D finite element model that completes the standard TRT analysis, estimating the thermal conductivity profile from a temperature profile along the borehole during the test. A highly conductivity layer was detected using this procedure, indicating the presence of ground water currents. The application of this methodology requires an extra resource effort regarding the TRT standard methodology because is needed a measurement of the borehole temperature profile and a more complex data analysis implemented in COMSOL. It should be noted that, in these previous works, the whole data recorded in during the research are not analysed; in this paper the complete data set are published.

The innovation introduced in this work is the presentation of a simple analysis methodology for standard thermal response tests performed under groundwater flow conditions, intended for engineering application, and based on finite line source model. This methodology is based on a phenomenological characterization of the impact of ground water advection in the estimation of ground thermal parameters extracted from line source model. The objective is that GSHE designers can know how the underground flow masks the result of the effective thermal conductivity and assess, based on this knowledge, what is the value that they will use for dimensioning, without the need for additional measurements to those made in standard TRT.

The structure of the paper is as follows: firstly, a description of the installation and the data collection system is done. Secondly, the characteristics of the three tests performed are presented and the raw data collected are analysed. Thirdly, an analysis of the effective thermal conductivity and the borehole resistance is carried out using traditional methodologies (finite line source and infinite line source analysis). Then, a modification of finite line analysis model to quantify the groundwater effects is presented and the data analysis redone using this new methodology. Finally, discussion of results and conclusions.

2. EXPERIMENTAL PLANT DESCRIPTION

2.1 Site geological information and characteristics of the borehole heat exchanger

The experimental installation is located at Universitat Politècnica de València and it was built on the first days of May 2010. The test site presents geological characteristics representatives of Valencia city with gravels, sands and clays as predominant materials and a high groundwater flow presence. During the drilling works, six layers were identified along the 40 meters drilled, as can be seen at the stratigraphic column represented in figure 1, a clay layer from 0 to 4 meters, a peat layer from 4 to 12 meters, a gravel with small round stones layer from 12 to 26 meters, another clay layer from 26 to 27 meter, a sand layer from 27 to 36 meters and a last layer of gravel with small round stones from 36 to 40 meters.

The facility consists of a borehole of 40 m. depth in which two independent PE-100 U-pipes of 40 mm diameter were introduced. Initially was planned both pipes with 40 m. depth, but after executing the drilling inserting a non-extracting metallic casing, a narrowing in the initial borehole diameter (160 mm) was observed at 30 m. depth, due to the casing installation, so it was decided to introduce a shorter U-pipe (installed depth 29 m.) and a longer U-pipe of 39 m. installed depth (figure 1). The space between the pipes and the casing was filled with a mixture of one part of bentonite and twelve parts of cement (CEMEX 32.5 raff) what is a very common commercial solution.

The installation is completed with a fixed thermo-hydraulic system that allows to carry out the heat injections test composed by a heating resistor of 3x1 kW/220 V, an electronic adjustable circulation pump and a 5-litre expansion tank (figure 2).

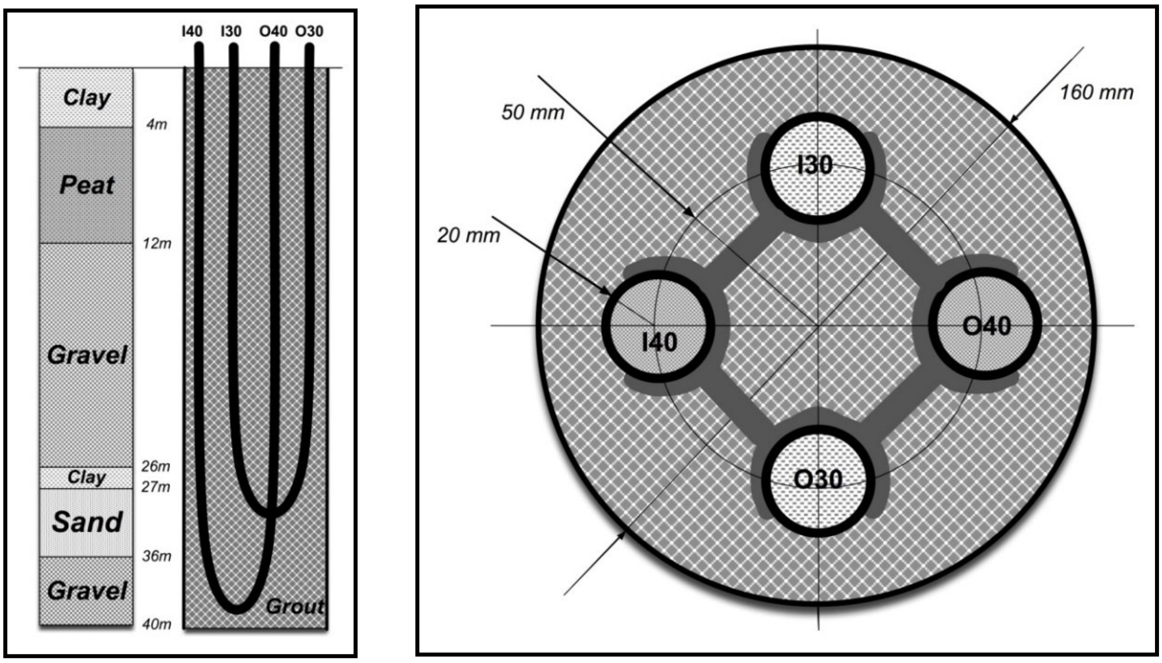

Fig. 1.- On the left, diagram showing the stratigraphic column of the borehole. On the right, diagram showing the location of both independent U-pipes, one 40 meters depth (I40, O40) and the other one 30 meters depths (I30, O30).

2.2 Monitoring system description

An equipment to control heat injection test was provided to the facility consisting of a flowmeter (accuracy of 1%) and temperature probes PT100 at input and output of the exchanger, connected to an acquisition system through a 4-wire 4–20mA loop of TC direct adjusted in a range from 0°C to 50°C. The temperature sensors (accuracy of 0,1 °C) were calibrated through a thermal bath and an electronic precision thermometer. Furthermore, an energy meter was employed for monitoring electric power source of the installation. The full system was managed from a PC with a touch screen and Internet access that performed acquisition and register of the data during the tests (figure 2).

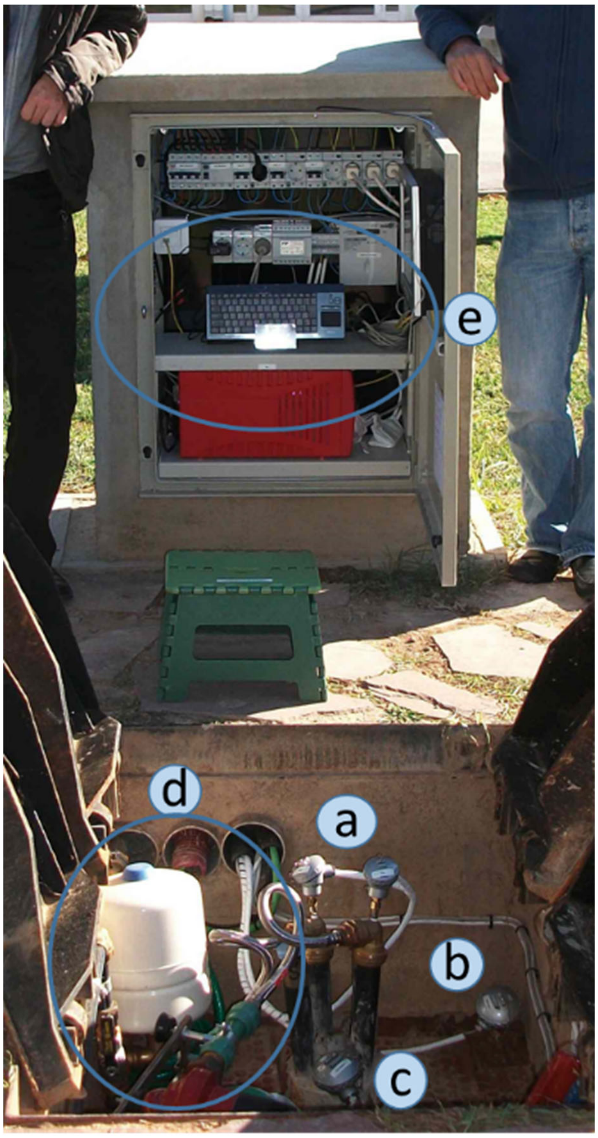

a) T_{in} , T_{out} temperature probes
b) Ground temperature probe
c) Borehole temperature probe
d) Hydraulic subsystem
e) Control and acquisition equipment

Fig. 2.- A picture of the borehole facility observing in the first place the borehole and the fixed thermo-hydraulic system and, in the background, the cabinet in which the data acquisition system is located.

In order to regularly measure the ground temperature, the longer U-pipe installed was prepared as explained in [45].

3. THERMAL RESPONSE TEST MEASUREMENTS

3.1 Ground temperature characterization

During the six months after the borehole execution, the ground temperature was characterized by inserting a calibrate sensor in the longer U-pipe, measuring the water temperature inside the pipes, in thermal equilibrium with the surrounding ground. The measurement procedure, repeated at least once a month, consisted in descending the sensor at prefixed depths, holding it in the position for 5 seconds for thermal stabilization and moving to the next depth. Between 1 and 4 meters depth, measures were taken every 0,5 meter, increasing that distance to 1 meter between 5 and 28 meters depth, reducing again the gap to 0,5 meters between 28,5 and 30,5 because at this depth there were problems during the casing installation as explained, and ending measuring every meter between 30,5 to 39 meters. Figure 3 shows the temperature profile depending on depth obtained. It is noted that the average temperature decreases around 2 ºC during the monitoring period and the undisturbed ground temperature is reached the fifth month after the installation works. In the graph the different ground layers observed during the drilling have been marked with bold vertical lines, no significant changes in the temperature profile between them are observed but it is remarkable the temperature peak observed at 30 m depth. This effect is because during the drilling works at this depth a fracture in the casing was observed so the grouting spilled into the ground increasing its thickness at this depth. According to this, it can be concluded that the ground temperature behavior in the first months after drilling works is due to the heat released during the grouting setting. Through this analysis, it was determined that the undisturbed ground temperature (T_0) at the test site is 20,12 ºC.

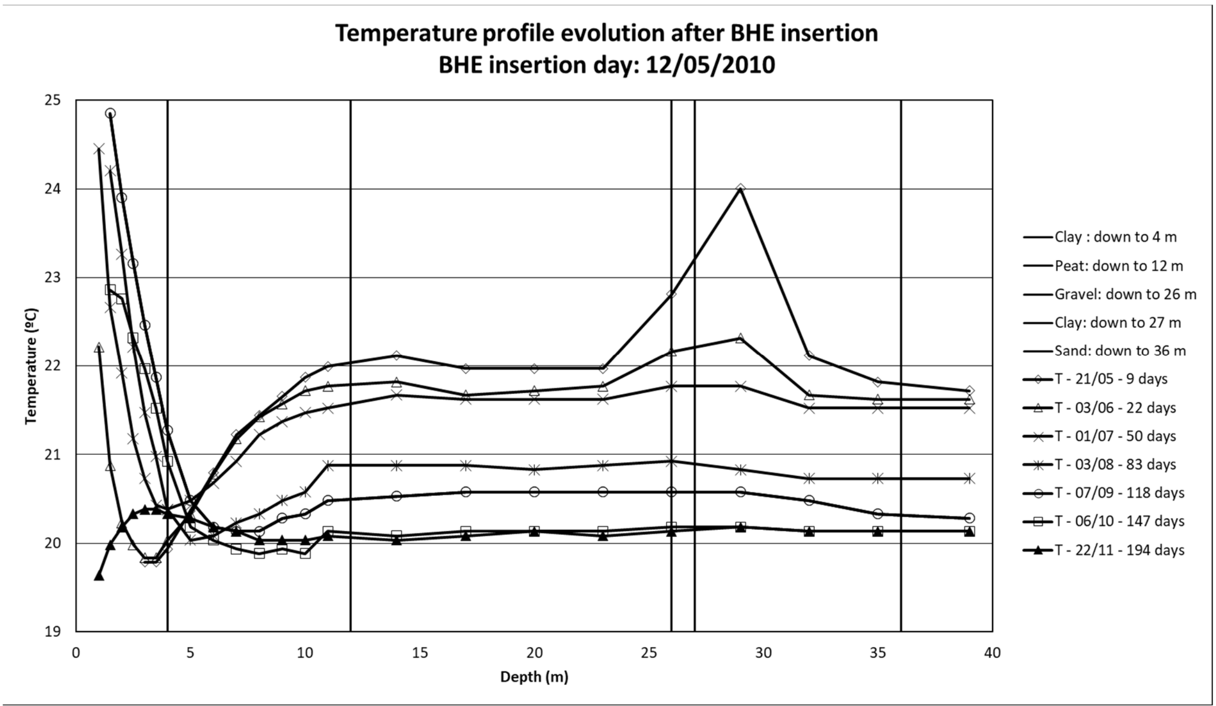

Fig. 3.- Ground temperature profile as a function of depth. Measures are given for the following 2010 dates: 21/05, 03/06, 01/07, 03/08, 07/09, 06/10 and 22/11.

3.2 Thermal response tests performed description

Once the undisturbed ground temperature was characterized, thermal response tests were started. Three heat injection tests were carried out in the shorter U-pipe during the following year and a half to the facility commissioning. The main characteristics of the test performed are shown in table 1.

Test	Dates	Duration (hours)	Data acquisition period (seconds)	Average injected thermal power (W)
2 kW	22/11/2010 – 26/11/2010	97,9	180	1637±51
3 kW	15/12/2010 - 20/12/2010	119,4	180	2449±67
1 kW	09/03/2011 – 30/03/2011	289,7	30	798±39

Table 1.- Duration of the TRT performed and average thermal power injected.

Figure 4 shows the measured data of the average fluid temperature circulating through the borehole heat exchanger for the three tests, $T_{ave} = (T_{in} + T_{out})/2$, as a function of time. In the following analysis of the data, presented in next sections, each test will be labeled 1, 2 or 3 kW tests, meaning the value of the heating resistors used, different from the actual injected thermal power. Data for the 1 kW test, with 21 days duration, will be analyzed only for the first 12 days.

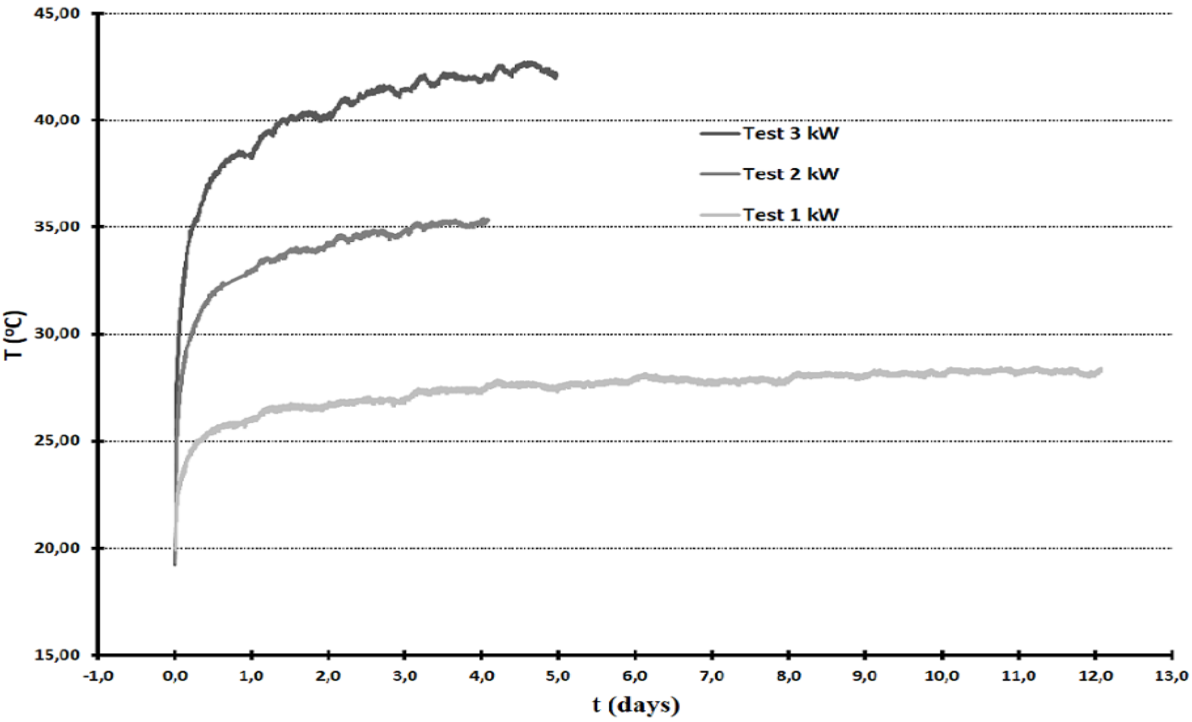

Fig. 4.- Average fluid temperature, T, as a function of time for the three performed test.

3.3 Ground temperature profile and recovery analysis

As mentioned above, the longer U-pipe was used to measure ground temperature profile before, during and after every test performed, inserting a calibrated temperature sensor in the pipeline, and measuring the temperature of the ground along the geothermal probe. The period in which ground temperature was recorded in each test is shown in table 2.

Test	Total period recorded	Duration of the recovery analysis period (days)
2 kW	22/11/2010 – 14/12/2010	18
3 kW	14/12/2010 – 10/01/2011	21
1 kW	02/03/2011 – 13/05/2011	44

Table 2.- Period of time in which ground temperature was recorded in each test.

Figures 5, 6 and 7 show the temperature values recorded before starting of the injection and during the thermal test execution. In all test carried out it can be seen that, before the injection, temperatures are quite constant, reaching the undisturbed ground temperature estimated from 7 meters depth. A similar trend is also observed in the temperature profile during the thermal test in the three power steps injected. Graphs present zones with higher heat absorption capacity attributable to the presence of groundwater (around 10 meters deep, around 19 meters and around 25 meters). In figure 5 (2 kW test) is not observed in detail the temperature decreasing at the depths of 19 and 25 meters because in this experiment the temperature measurement was done each 3 meters between 10 and 39 meters. Due to the rapid drop of the temperature observed between 25 and 30 meters deep and to perform a better analysis, in the following tests (figures 6 and 7), the temperature was recorded every meter depth to observe the behaviour in the different ground layers, clearly observing the zones with higher heat absorption capacity.

The different behaviour between ground layers it is noted as well in the monitoring of the ground several days after the completion of the thermal response test (figures 8, 9 and 10), where same depths show a faster recovery. It is observed that the ground recovery period to return to the undisturbed ground temperature is more than 15 days for all injected thermal power values due to the long test period.

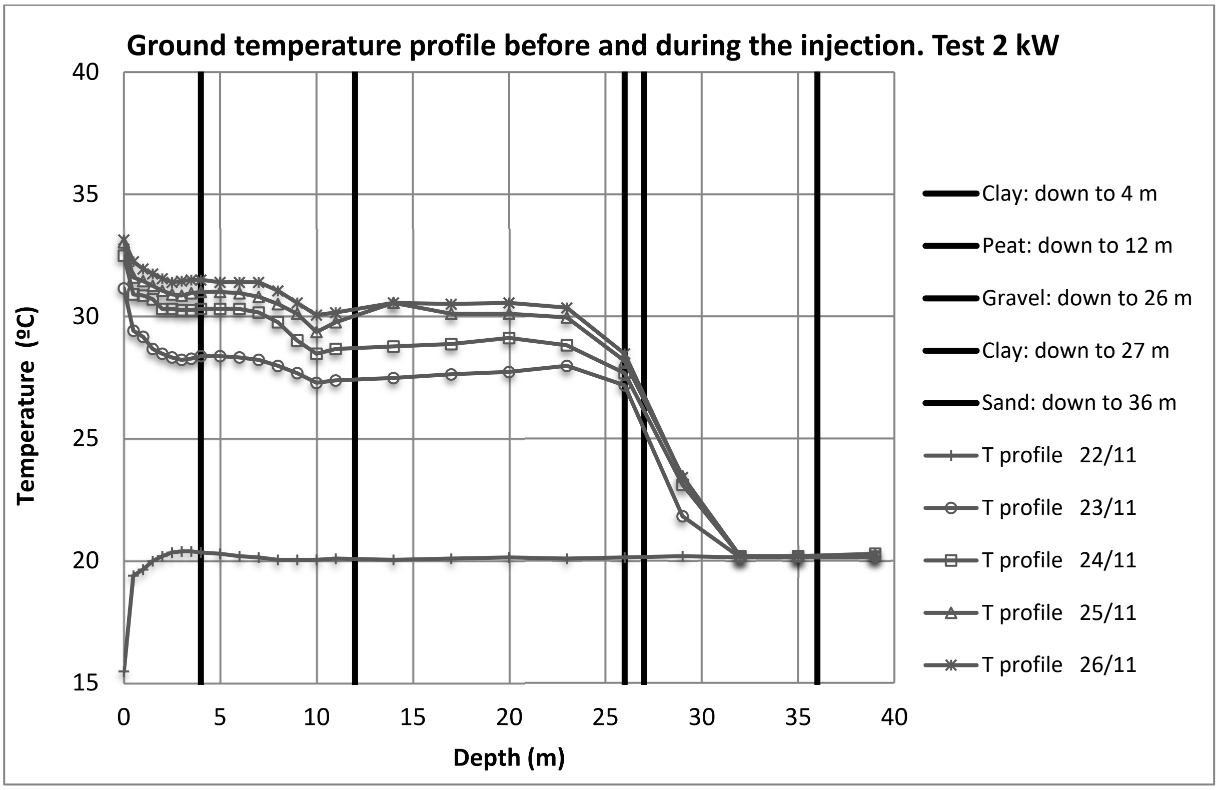

Fig. 5.- Ground temperature profile as a function of depth just before (22/11) and during the injection for the 2 kW test.

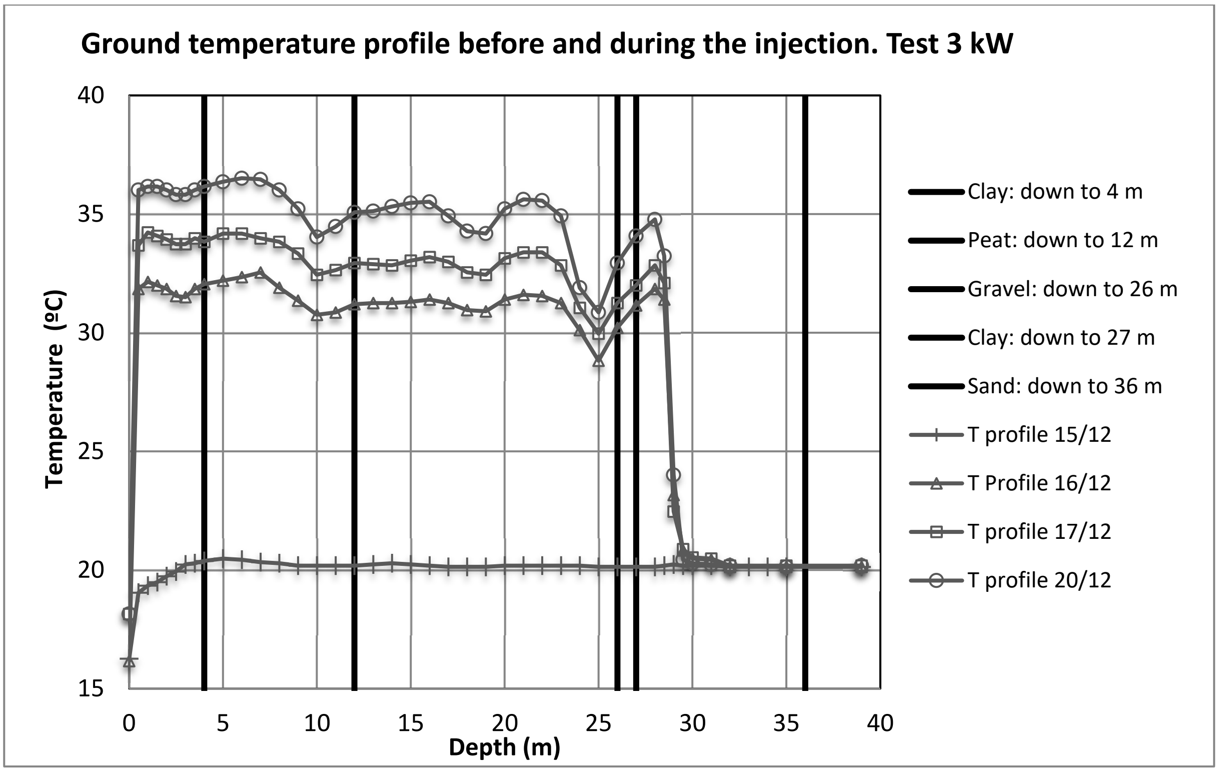

Fig. 6.- Ground temperature profile as a function of depth just before (15/12) and during the injection for the 3 kW test

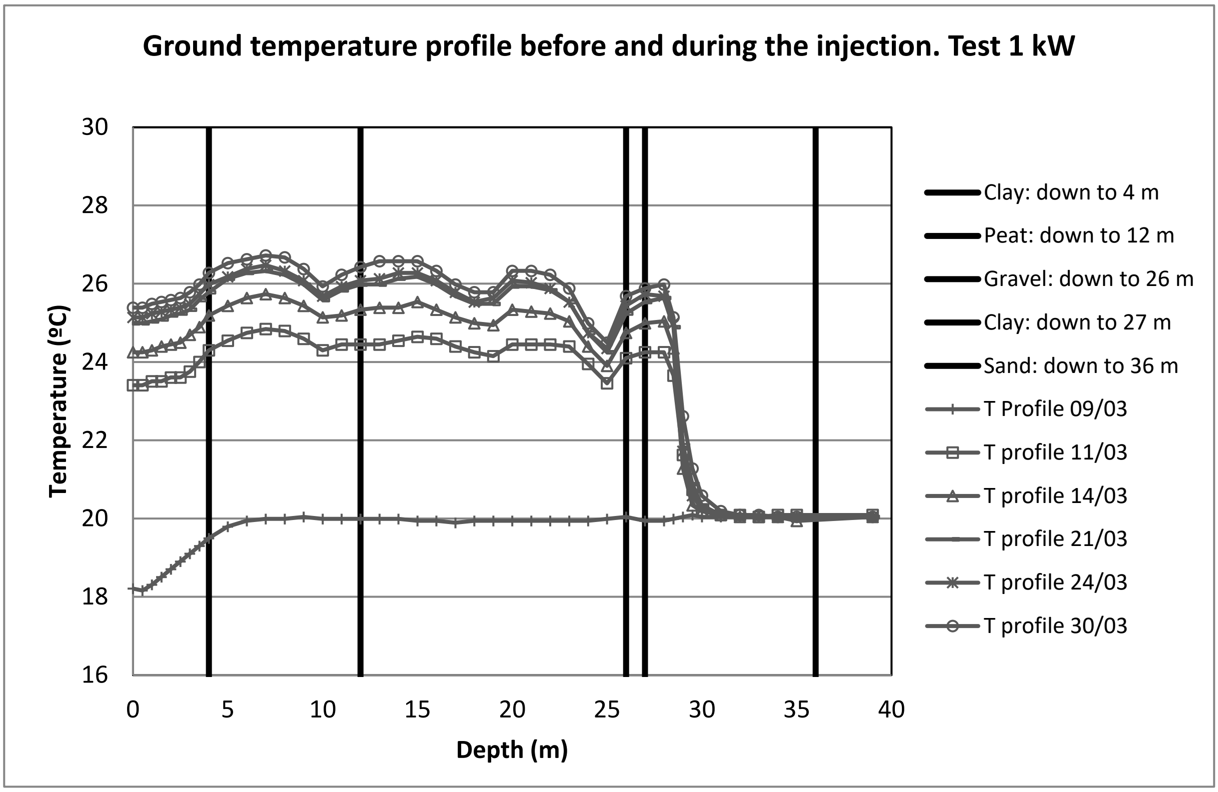

Fig. 7.- Ground temperature profile as a function of depth just before (09/03) and during the injection for the 1 kW test.

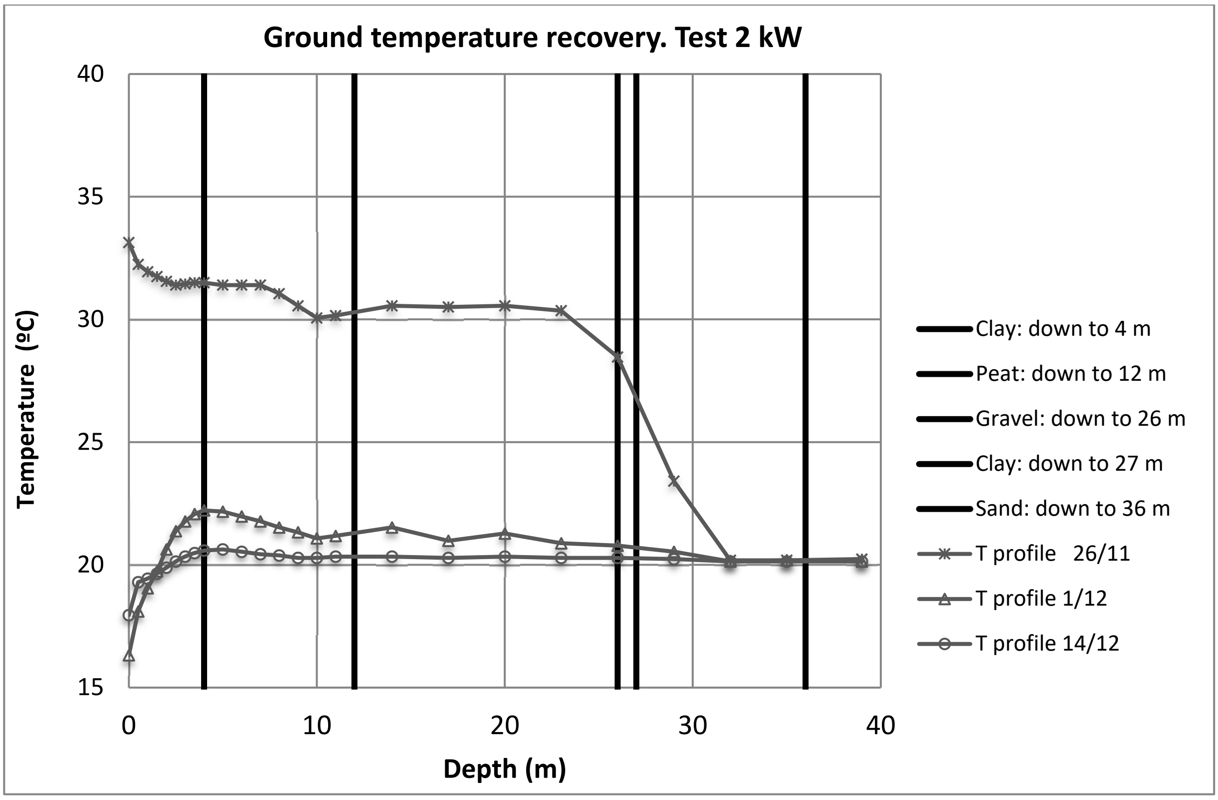

Fig. 8.- Ground temperature profile as a function of depth at the end of the the injection (26/11) and after for the 2 kW test.

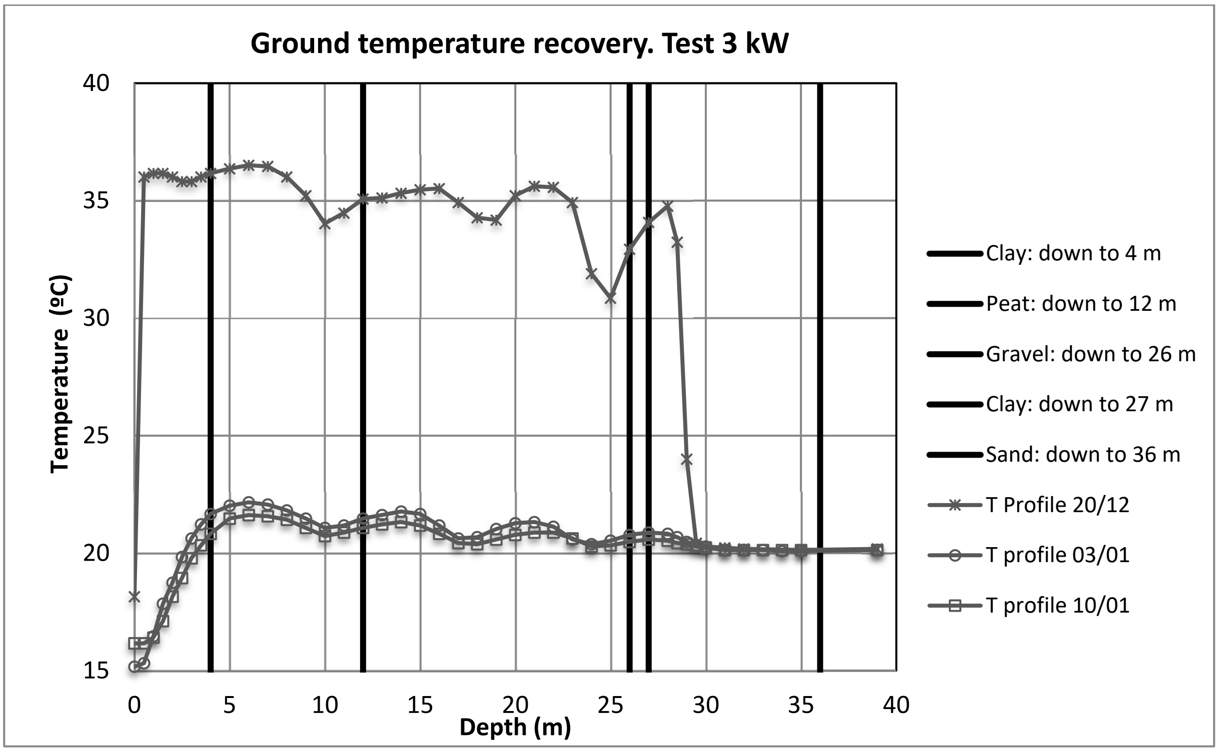

Fig. 9.- Ground temperature profile as a function of depth at the end of the the injection (20/12) and after for the 3 kW test.

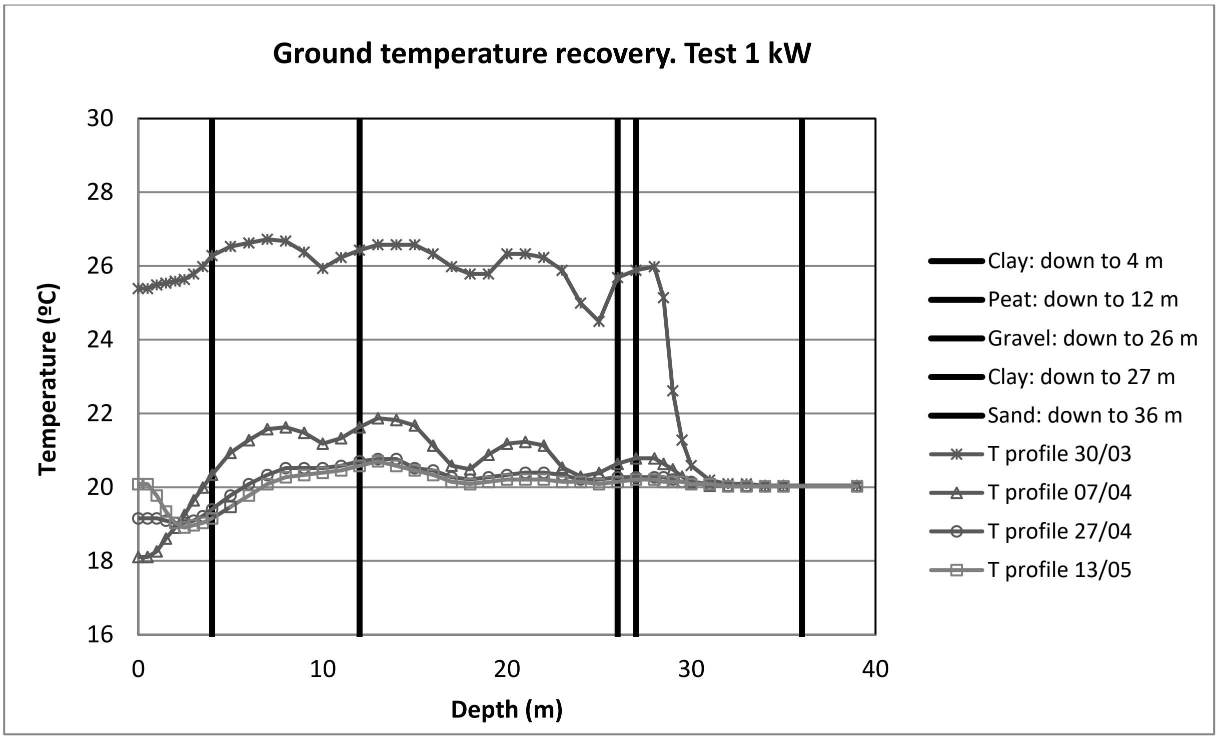

Fig. 10.- Ground temperature profile as a function of depth at the end of the the injection (30/03) and after for the 1 kW test.

4. DATA ANALYSIS

The purpose of this work is to obtain the effective ground thermal conductivity value under groundwater conditions from data recorded on standard TRT, without the addition of new measurements to characterize the subsoil layers, developing an effective model based on line source analysis. This model is selected because is the most widely used in TRT analysis and is recommended by international standards to find an accurate estimation of three parameters approximately describing the thermal behaviour of the ground under consideration and needed to design a ground coupled heat pump installation. These parameters are the undisturbed ground temperature, T_0, the effective ground thermal conductivity, λ, and the borehole thermal resistance, R_b. Variation of the line source model is carried out adding a new effective parameter to incorporate the impact of ground water flow on ground thermal properties.

Line source analysis assumes that the borehole heat exchanger behaves as a linear heat source emitting constant thermal power. This analysis also assumes that the ground is a homogeneous infinite medium whose thermal behavior is characterized by its thermal conductivity, λ, and its thermal diffusivity, α. Considering the source with an infinite length, meaning that the borehole depth, L, is much bigger than the borehole radius, r_b, the solution of this thermal problem gives the temperature of the ground as a function of the radial coordinate, and the time, t:

$$T(r,t) = T_0 - \frac{Q_z}{4\pi\lambda} Ei\left(-\frac{r^2}{4\alpha t}\right) \quad (1)$$

Where T_0 in the undisturbed ground temperature and Q_z the constant heat power injected to the ground per length unit. Symbol Ei represents the Euler integral. For sufficiently large times this expression can be approximated by:

$$T(r,t) \approx T_0 + \frac{Q_z}{4\pi\lambda}\left\{ln\frac{4\alpha t}{r^2} - \gamma + O\left(\frac{r^2}{4\alpha t}\right)\right\}, \qquad for \qquad \frac{4\alpha t}{r^2} \gg 1 \quad (2)$$

This expression is usually used to estimate the value of the temperature at the borehole radius, r_b, during a Thermal Response Test:

$$T(r_b,t) = T_b(t) = T_0 + \frac{Q_z}{4\pi\lambda}\left\{ln\left(\frac{t}{t_b}\right) - \gamma\right\}, \qquad for \qquad t \gg t_b = \frac{r_b^2}{4\alpha} \quad (3)$$

Then, borehole thermal resistance, R_b, is defined to model the inner problem of heat transfer inside the BHE, relating the average of the fluid temperature, $T_{ave}(t)$, with the temperature at the borehole surface, $T_b(t)$, through the expression:

$$T_{ave}(t) = T_b(t) + Q_z R_b \quad (4)$$

Thermal response tests measure inlet, T_{in}, and outlet temperature, T_{out}, to the borehole heat exchanger, as well as fluid mass flow, $\dot{m}$, allowing calculating average fluid temperature, T_{ave}, and thermal power injected to the ground, Q_z, through:

$$T_{ave} = \frac{T_{in}+T_{out}}{2} \qquad\qquad Q_z = \frac{\dot{m}\, C_p\, (T_{in}-T_{out})}{L} \quad (5)$$

If the assumptions of the infinite line source analysis are reasonable for the thermal response test under consideration, then average fluid temperature will follow the expression:

$$T_{ave}(t) = T_0 + Q_z R_b + \frac{Q_z}{4\pi\lambda}\left\{ln\left(\frac{t}{t_b}\right) - \gamma\right\} \quad (6)$$

Usual analysis plots data of average fluid temperature against logarithm of time. Then, a linear behaviour of these experimental data will confirm the assumptions of the infinite line source, extracting ground thermal properties and borehole resistance from the slope, a, and the intercept, b, of the linear fit:

$$a = \frac{Q_z}{4\pi\lambda} \qquad b = T_0 + Q_z\left(R_b - \frac{\ln(t_b)-\gamma}{4\pi\lambda}\right) \tag{7}$$

From the slope, a, effective thermal conductivity of the ground is estimated, $\lambda = Q_z/4\pi a$, and from the intercept, b, a relationship between the undisturbed ground temperature, T_0, the ground thermal diffusivity, α (included in the time constant $t_b = r_b^2/4\alpha$) and the borehole thermal resistance, R_b, is found. If a measurement of the undisturbed ground temperature is done and an estimation of ground thermal diffusivity is available, then borehole thermal resistance can be calculated from expression:

$$R_b = \frac{b-T_0}{Q_z} + \frac{\ln(t_b)-\gamma}{4\pi\lambda} \tag{8}$$

In the three thermal response tests analysed in this work an accurate measurement of the undisturbed ground temperature was done and a previous estimation of ground thermal diffusivity is available, so borehole thermal resistance can be calculated. As the three tests were executed at different injected powers, it is convenient to choose appropriate variables allowing comparing the three tests in a clear way, being a suitable choice f_0 and τ, defined as:

$$f_0 = \frac{T_{ave}(t)-T_0}{Q_z} \qquad and \qquad \tau = \frac{ln\left(\frac{t}{t_b}\right)-\gamma}{4\pi} \tag{9}$$

because the relation between these two variables predicted by the infinite line source approach, given by:

$$f_0 = R_b + \frac{\tau}{\lambda} \tag{10}$$

is independent of the injected power. Therefore, calculating variables f_0 and τ from the experimental data of the three response tests, and plotting f_0 against τ, all experimental points have to describe a line whose intercept is the borehole thermal resistance and its slope the inverse of the effective thermal conductivity. First analysis of TRT data has been done using this methodology. In addition, a second analysis with the purpose of evaluating the effect on the estimates of a finite line source has also been done.

The solution of the heat transfer problem between the borehole heat exchanger and the ground, considering a finite borehole length, is dependent of the vertical coordinate. Therefore, the temperature at the borehole radius depends on this coordinate and the analysis of ground thermal response test data is more elaborated. In this contribution, the procedure adopted to consider finite length effects uses the average of the temperature at the borehole radius along the whole length, L, of the borehole heat exchanger. The final expression to estimate the temperature at the borehole radius is:

$$T(r_b,t) = T_0 + \frac{Q_z}{4\pi\lambda}\left\{ln\left(\frac{t}{t_b}\right) - \gamma - \left(\frac{3}{\sqrt{\pi}}\left(\sqrt{\frac{t}{t_L}} - \left(\frac{r_b}{L}\right)^2\sqrt{\frac{t_L}{t}}\right) - 3\frac{r_b}{L}\right)\right\} \tag{11}$$

where t_L is a characteristic time scale associated to the borehole length:

$$t_L = \frac{L^2}{4\alpha} \tag{12}$$

This expression for the temperature at the borehole radius was calculated in [20] as a series expansion of the exact solution, averaged along the length of the BHE, in variables t_L and r_b/L. Note that if the length L is considered infinite the previous solution for the infinite approach is recovered. Also, note the meaning of the infinite line approach, the length of the borehole, L, is much bigger than the borehole radius, r_b.

Then, considering the relation between the average fluid temperature and temperature at the borehole radius through the borehole thermal resistance, finite line source approach predicts a temporal evolution of the average fluid temperature given by expression:

$$T_{ave} = T_0 + Q_z R_b + \frac{Q_z}{4\pi\lambda}\left\{ ln\left(\frac{t}{t_b}\right) - \gamma - \left(\frac{3}{\sqrt{\pi}}\left(\sqrt{\frac{t}{t_L}} - \left(\frac{r_b}{L}\right)^2 \sqrt{\frac{t_L}{t}}\right) - 3\frac{r_b}{L}\right)\right\} \quad (13)$$

To analyse TRT data including finite lengths effects is also convenient a suitable choice of variables to compare the three tests, being in this case f_0 and τ–$\Delta\tau$, with f_0 and τ as defined previously and Δτ defined as:

$$\Delta\tau = \frac{1}{4\pi}\left\{\frac{3}{\sqrt{\pi}}\left(\sqrt{\frac{t}{t_L}} - \left(\frac{r_b}{L}\right)^2 \sqrt{\frac{t_L}{t}}\right) - 3\frac{r_b}{L}\right\} \quad (14)$$

because the relation between these f_0 and τ–Δτ predicted by the line source approach, given by:

$$f_0 = R_b + \frac{\tau - \Delta\tau}{\lambda} \quad (15)$$

is again independent of the injected power. Therefore, as with the infinite line approach, the experimental values of f_0 represented against τ–$\Delta\tau$ must describe a line whose intercept is the borehole thermal resistance and its slope the inverse of the effective thermal conductivity.

Figure 11 is elaborated to show the accuracy of the finite line source prediction, equations 13 and 15, to describe the behaviour of the experimental data acquired during the execution of the three thermal response tests carried out. For calculating f_0 (from equation 9) variable the values of the undisturbed ground temperature, T_0, and the average injected thermal power, Q_z, are needed. Undisturbed ground temperature has been accurately measured resulting the value T_0=20,12 ºC. Average injected thermal power per length unit, Q_z, is calculated from the experimental measurements of average injected power shown in table 1, resulting the values presented in table 3. And for calculating τ and $\Delta\tau$ (from equations 9 and 14) the values of the borehole radius (r_b=0,08 m), borehole depth (L=29 m) and the ground thermal diffusivity, α, are needed. An estimation of the ground thermal diffusivity is available from previous research works, from reference [46], in which a comparison between design and actual energy performance of a HVAC-ground coupled heat pump system located 500 m. away from the test site is presented, reporting values for ground thermal conductivity λ=1,43 W/mK, ground volumetric thermal capacity C_v=2400 kJ/m^{3}K and ground thermal diffusivity $\alpha=\lambda/C_v$=0,0000006 m^{2}s^{-1}. This constant value of ground thermal diffusivity, α, is the one used along the present analysis.

Figure 11 represents the values of $f_{0i}=f_0-R_{b0i}$ against the values of τ–$\Delta\tau$ calculated from these experimental data, with R_{b0i} the borehole thermal resistance estimated for the test i (i=1,2,3) at the beginning of each test. If FLS prediction applies, then all experimental points will show a linear behaviour with 0 intercept and slope the inverse of the effective thermal conductivity. The choice of variable f_{0i} for the vertical axis of figure 11 is done to enhance clarity of the comparison between the three tests. A linear fitting between f_0 and τ–$\Delta\tau$, of the data from values of τ–$\Delta\tau$ starting in 0,03 (equivalent to 1,9 hours) and finishing in 0,07 (equivalent to 3,2 hours) for the three tests, gives the values included in table 3 for the intercept and the slope. Then, R_{b01}=0,094 mK/W, R_{b02}=0,117 mK/W and R_{b03}=0,114 mK/W.

Test	Injected power Q_z (W/m)	Intercept (m K/W)	Slope (m K/W)	C.C.
1 (1 kW)	27,72	0,094	0,564	0,974

2 (2 kW)	56,45	0,117	0,564	0,995
3 (3 kW)	84,44	0,114	0,560	0,994

Table 3.- Values of intercept, slope and correlation coefficient (C.C.) for the linear fitting of f_0 against $\tau\text{–}\Delta\tau$ for data of $\tau\text{–}\Delta\tau$ between 0,03 and 0,07.

A first estimation of the effective ground thermal conductivity and borehole thermal resistance could be obtained from de data of table 3. The estimate of the ground thermal conductivity is the inverse of the slope so, considering the results of the three tests and averaging, the estimate will be λ =1,777±0,007 W/mK. And the estimate for the borehole thermal resistance is the intercept so, averaging, R_b=0,108±0,012 mK/W. It is remarkable that the three linear fits are very accurate with correlation coefficients very close to the unity. This fact is reflected in figure 11, in which the variables f_{0i} for the three tests calculated from the experimental data are shown (light grey line for the 1 kW test, dark grey line for the 2 kW test and black line for the 3 kW test), as the good agreement in the range of $\tau\text{–}\Delta\tau$ starting in 0,03 and finishing in 0,07 between the experimental points and the linear tendency described by the dashed grey line, plotted using the average of the slopes included in table 3, 0,563 mK/W. Nevertheless, this procedure is done for very early times and line source approach is valid for values of time much bigger than $t_b = r_b^2/4\alpha$, corresponding this value to t_b=0,74 h, close to the fitting range, from 1,9 hours to 3,2 hours. So, this first estimation is not completely valid but serves to understand the further development.

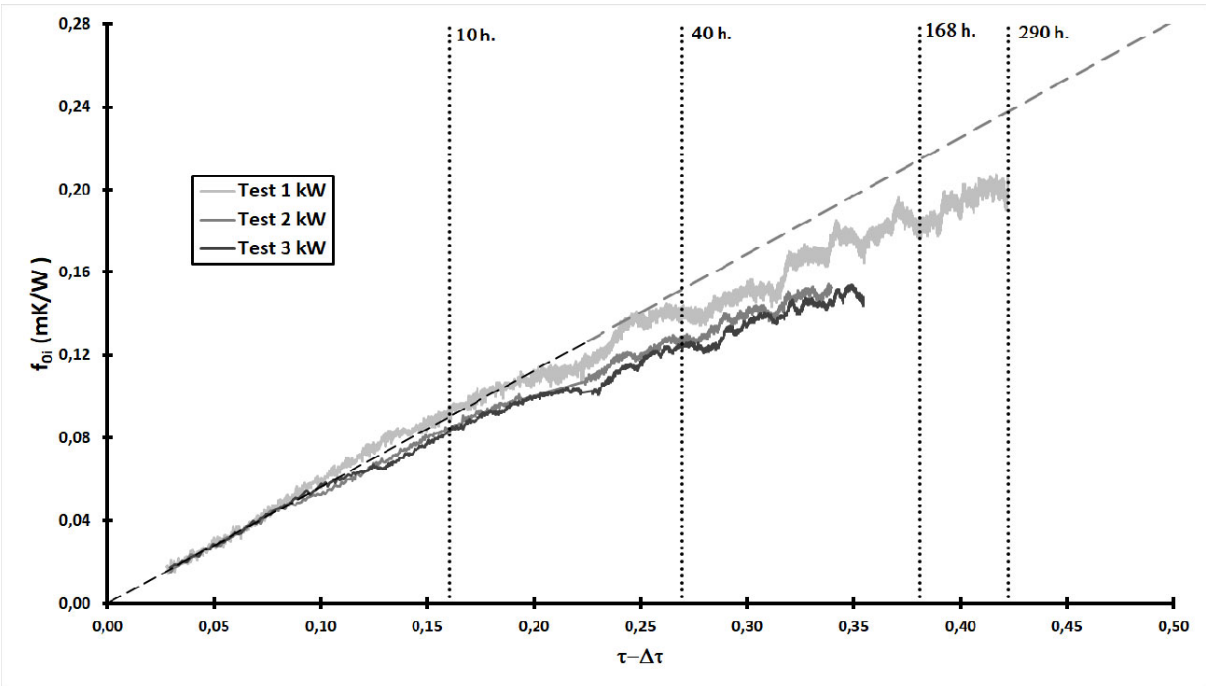

Fig. 11.- The values of f_{0i}=f_0-R_{b0i} against the values of $\tau\text{–}\Delta\tau$ for the test i (i=1,2,3) are represented.

A qualitative analysis of the data presented in figure 11 drives to the following conclusions. First, after a $\tau\text{–}\Delta\tau$ value of approximately 0,10 (corresponding to 4,64 hours) the data for the different tests starts to split, drawing curves in which the slope decrease with time (for long time periods) and this decrease depends on the thermal power injected, being this decrease greater when the injected thermal power is greater. This decrease can also be understood as dependency with the difference between the average temperature of the injected fluid and that of the undisturbed ground. Second, the three curves do not describe a linear behaviour in the variables represented as predicted by the line source approach. This fact can be clearly seen comparing each experimental test curve with the dashed line representing the behaviour of the three tests at its beginning (values of $\tau - \Delta\tau$ from 0,03 to 0,07). And third, local oscillations are observed in the three tests, short sections in which the slope can increase or decrease. The same oscillations are observed in the three tests, showing very similar patterns at the same values of $\tau - \Delta\tau$. Then, these oscillations are a physical effect, which can be interpreted as the appearance (conductivity increases, slope decreases) and disappearance (conductivity decreases, slope increases) of groundwater, phenomena activated by the injection of thermal power to the ground.

Although the qualitative analysis of the TRT data indicates slight discrepancies with line source prediction, it is interesting to analyse it with standard line source methodology. The data of the three tests have been fitted to the prediction of the infinite line source theory (equation 10) and to the prediction of the finite line source theory (equation 15) for different ranges of time. First range of time analysed is from t=10 to t=40 hours, starting from a value satisfying the constraint given in equation 3, $t \gg t_b = 0{,}7$ h, and for a time length of 30 hours. Estimates for the thermal conductivity and borehole thermal resistance for this fitting range, both analysis procedures and the three tests are included in table 4. First conclusion obtained after looking at these fitting results is that finite line source analysis estimates slightly lower values for both, thermal conductivity and borehole thermal resistance, than infinite line source analysis, with no significant differences. So, finite length effects could be neglected in this case. Second conclusion is that the three tests behave almost linearly in this fitting range, with correlation coefficients very close to the unity. Nevertheless, and as third conclusion, the estimates for thermal conductivity and borehole resistance differ considerably, being higher as the injected power increases. If the average of the three estimates is considered, and as error half the highest distance between them, then the prediction for thermal conductivity is $\lambda = 2{,}445 \pm 0{,}336$ W/mK (an error around 14%) and $R_b = 0{,}128 \pm 0{,}011$ mK/W (an error around 9%). Errors are associated to the discrepancy between the actual physical phenomena and the model that is not enough to describe them. This lack of accuracy reflects the fact that groundwater effects are already relevant in this fitting range, appearing in this line source methodology as an increasing dependency of the estimates for thermal conductivity and borehole resistance with the injected power. This dependency of the estimates does not mean that both depend on the injected power, it means that the line source approach is not able to describe groundwater effects and, then, these are artificially incorporated as estimates depending on input parameters as the injected power.

Second range of time analysed for tests 2 and 3 are from t=40 hours until the end of the proof, t=98 hours for test 2 and t=120 hours for test 3. For test 1, a much longer experiment, two more ranges are analysed, a second range, from t=40 hours until t=168 hours, and a third range, from t=168 hours until the end, in this case t=290 hours. Estimates for the thermal conductivity and borehole thermal resistance for these fitting ranges, both analysis procedures and the three tests are included in table 4.

		Finite line source analysis			Infinite line source analysis		
Fitting range	Test	R_b (mK/W)	λ(W/mK)	C.C.	R_b (mK/W)	λ(W/mK)	C.C.
10-40 hours	1	0,107	2,065	0,972	0,108	2,093	0,972
	2	0,139	2,530	0,992	0,140	2,563	0,992
	3	0,139	2,738	0,981	0,140	2,774	0,981
40-168 hours	1	0,104	2,119	0,963	0,107	2,176	0,963
40-98 hours	2	0,147	2,768	0,955	0,149	2,831	0,954
40-120 hours	3	0,144	2,883	0,961	0,145	2,953	0,961
168-290 hours	1	0,099	2,117	0,855	0,104	2,208	0,854

Table 4.- Estimates for the thermal conductivity and borehole thermal resistance for several fitting ranges, finite line source analysis and infinite line source analysis, and the three thermal response tests are included. Correlation coefficients (C.C.) of each fitting are also included.

After looking at these fitting results for these second and third ranges, similar conclusions as the ones reached for the first range are achieved. No significant difference is found between estimates from infinite line source and from finite line source methodology. Again, slightly lower estimates are obtained using finite line source analysis with very small quantitative significance of the differences. The three tests still behave linearly but correlation coefficients are lower than in first range, being more appreciable the discrepancies of the data with the line source prediction. This means that groundwater effects also become higher with time. Estimates for thermal conductivity and borehole thermal resistance achieve values higher than in first range, so it seems that both parameters get higher with higher injected power and with time.

From the qualitative and quantitative analysis of the three tests, two effects not described by the line source approach are identified, both produced by groundwater advection mechanisms. First one, observed for long time periods, is the increasing of the estimate for the effective thermal conductivity as well as the borehole thermal resistance, being this increase greater when the injected thermal power is greater. And second one, local oscillations in short time ranges of the data, in which the slope, whose inverse is the estimate of thermal conductivity, can increase or decrease. These short time oscillations can be interpreted as the appearance (conductivity increases, slope decreases) and disappearance (conductivity decreases, slope increases) of groundwater, phenomena activated by the injection of thermal power to the ground.

One of the purposes of this research work is finding a phenomenological quantitative description of the observed new effects. In particular, the long-term effect driving to the unphysical result of a thermal conductivity depending on time and injected power. A phenomenological parametrization of this effect can be obtained with an expression for the effective thermal conductivity depending on the difference between the average fluid temperature, T_{ave}, and the undisturbed ground temperature, T_0, as the following one:

$$\lambda = \lambda_0 \left(1 + x \frac{T_{ave} - T_0}{T_0}\right) \qquad (16)$$

Where the new parameter, x, quantifies the effect produced by underground water currents. Both observed dependencies, with time and with injected thermal power, can be described with this approach. With this parametrization, groundwater effects are phenomenologically integrated in the line source approach as a more complex definition of effective thermal conductivity. Introducing this new definition for λ given in equation 16 in the finite line source equation 15 it is obtained:

$$[f_0 - R_b]\left(1 + x\frac{T_{ave}-T_0}{T_0}\right) = \frac{\tau-\Delta\tau}{\lambda_0} \tag{17}$$

Expression representing the new prediction of this improved line source approach for the thermal response test data. Defining de quantity $f_{GW}(x)$ as:

$$f_{GW}(x) = [f_0 - R_b]\left(1 + x\frac{T_{ave}-T_0}{T_0}\right) \tag{18}$$

Final expression for this new prediction is formally identical to the previous one, equation 15, just changing f_0-R_b by f_{GW}:

$$f_{GW}(x) = \frac{\tau-\Delta\tau}{\lambda_0} \tag{19}$$

Note that this expression is developed on top of the finite line source approach but, if infinite line source is the one involved, the same expression is valid just eliminating the term including finite length effects, $\Delta\tau$.

Figure 12 is elaborated to check if this new expression predicts the experimental data from the three thermal response tests. The quantity f_{GW} is plotted against the variable τ–$\Delta\tau$, if the prediction is correct then data will behave linearly and at the same position for the three sets of data. To calculate the values for f_{GW} estimations for R_b and x are needed. In figure 12 values for R_b are the same as the ones used in figure 11, R_{b01}=0,094 mK/W, R_{b02}=0,117 mK/W and R_{b03}=0,114 mK/W, corresponding to a fit of the very early data of the test. Then, actual definition for the vertical variable presented in figure 12 is:

$$f_{GWi}(x) = [f_0 - R_{bi}]\left(1 + x\frac{T_{ave}-T_0}{T_0}\right) \tag{20}$$

And the prediction to be observed:

$$f_{GWi}(x) = \frac{\tau-\Delta\tau}{\lambda_0} \tag{21}$$

Linear fittings of the variable$f_{GWi}(x)$ against the variable τ–$\Delta\tau$, in the range between 10 hours and the end of each test (290 hours for test 1 kW, 98 hours for test 2 kW and 120 hours for test 3 kW), for different values of x are performed. The one presented in figure 12 corresponds with the values of x minimizing the differences between the three estimates of λ_0. The values obtained are $\lambda_{0\text{-}1kW}$*=2,107 W/mK*, $\lambda_{0\text{-}2kW}$*=2,166 W/mK* and $\lambda_{0\text{-}3kW}$*=2,083 W/mK* for the optimum value of x*=3,4*. Averaging the three values, an estimation for this parameter will be λ_0*=2,119 W/mK*, and taking as error half the maximum difference between them, $\Delta\lambda_0$=0,042 W/mK. In long time periods, figure 12 show a clearer linear tendency of the variable $f_{GWi}(x)$ as a function of the variable τ–$\Delta\tau$, in the time range analysed, 10 to 290 hours. This fact is supported by the correlation coefficients of each fitting, very close to the unity, and better than the ones obtained using line source approach (included in table 4). Values for correlation coefficients are now: $C.C._{Test\ 1kW}$=0,987, $C.C._{Test\ 2kW}$=0,991 and $C.C._{Test\ 3kW}$=0,991. Intercepts of the fittings are slightly different from cero, then, a small correction to each value of the estimate for borehole resistance is obtained, driving to the values R_{b1}=0,117 mK/W, R_{b2}=0,141 mK/W and R_{b3}=0,137 mK/W. Averaging the three values an estimation for this parameter will be R_b*=0,133 mK/W*, and taking as error half the maximum difference between them, ΔR_b=0,012 *mK/W*.

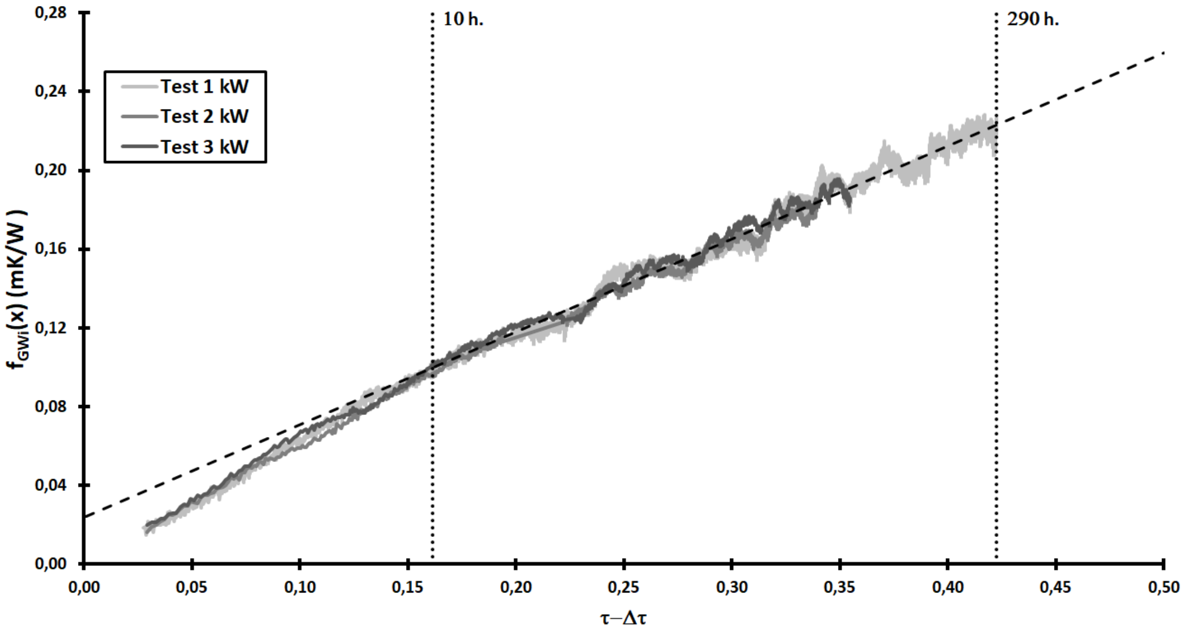

Fig. 12.- The values of f_{GWi} against the values of τ–$\Delta\tau$ for the test i (i=1,2,3) are represented

Together with the values of $f_{GWi}(x)$ figure 12 also includes a dashed line representing the linear prediction obtained, line with slope $m=1/\lambda_0$=0,472 mK/W and intercept a=0,024 mK/W. The agreement is quite well in the long range, describing appropriately experimental data, nevertheless, showing the short time oscillations with the really interesting fact that these oscillations are almost equal for the three tests when variables are presented as defined in horizontal and vertical axis of figure 12: experimental data of the three tests almost overlap.

The choice of the fitting range for this first analysis has been done with the criteria of starting at a point in which finite line source approach is valid and ending at the end of the acquisition period. Another interesting choice is a typical range of a standard test, starting at a point in which finite line source approach is valid and ending two days after. This fit has been also done, from 10 hours to 57,2 hours, including the results in table 5 (also in this table results for previous fit from 10 hours to the end are included). No significant differences between both fitting ranges are observed, being all estimates compatibles, and correlation coefficients very close to the unity.

Finally, another interesting choice for fitting range is an early starting (although is a range in which finite line source approach starts to be valid) because figure 11 showed that ground water effects appear even in this range. So, a fitting analysis starting in 1,9 hours has been done with to ends, one the end of the test and the other 57,2 hours. Results are included in table 5, showing, as expected, a slight decreasing of the estimate for parameter λ_0, but with very good agreement between the model and experimental results.

		Finite line source analysis including ground water effects		
Fitting range	Test	R_b (mK/W)	λ_0(W/mK)	C.C.
10 hours-end	1	0,117	2,107	0,987
	2	0,141	2,166	0,991
	3	0,137	2,083	0,991
10 hours-57,2 hours	1	0,119	2,145	0,972
	2	0,139	2,117	0,991
	3	0,140	2,146	0,984
1,9 hours-end	1	0,114	2,066	0,991
	2	0,132	2,027	0,995
	3	0,131	2,001	0,995
1,9 hours- 57,2 hours	1	0,109	1,977	0,989
	2	0,128	1,954	0,996
	3	0,129	1,964	0,994

Table 5.- Estimates for λ_0 and R_b using the finite line source analysis including ground water effects for the three thermal response tests and different ranges are included. Correlation coefficients (C.C.) of each fitting are also included.

5 DISCUSSION

The integration of the groundwater phenomenon in the finite line analysis model aims to reasonably describe the behaviour observed in the thermal response tests performed by the usual analysis methods. That is, a non-real increase in the value of the thermal conductivity depending on time and injected power, an augment that has also be assumed in the behaviour of the ground thermal heat capacity, thus keeping the thermal diffusivity constant. The introduction of a more complex definition of effective thermal conductivity in the model through a parameter that quantifies the effect produced by underground water currents allows to estimate the true value of the thermal conductivity, λ_0, regardless the power injected or the time elapsed in the test, as observed in the table 5. This is due to the fact that the effective thermal conductivity is divided into two terms, one static which is called "true value" because is unaffected by underground flow and another dynamic that depends on time and is characterized by parameter x. The differences in thermal conductivity values obtained both in different power injections and in different time intervals considered are less than 0,083 W/mK, that represents 4% of the average thermal conductivity value, while in the analysis performed through conventional finite line source method, table 4, this maximum difference is around 0,7 W/mK, that is 28% of the average thermal conductivity value estimated. This improvement in the results of the model analysis proposed is even more notable in the typical range time of a standard test, from 10 hours to 57,2 hours, since in this case the difference between the values obtained represents 1,4% of the average thermal conductivity whereas in conventional analysis, interval from 10 to 40 hours, this difference is 27%.

This model has been applied using three injection pulses although, generally, thermal response test is performed only with an injection pulse but this does not exclude the application of this methodology because, in this case, the procedure to follow will be to find the parameter x that maximizes the correlation coefficient. In this way, the objective of the work to simplify the analysis methodology for the thermal response tests performed under groundwater flow conditions intended for engineering applications is achieved.

In the analysis of the effective thermal conductivity value performed using traditional methodologies (finite line source and infinite line source analysis), figure 11 and table 4, it is noted that, in all cases, thermal conductivity value increases with the duration of the thermal power injection, being this augment smaller at low powers (test 1 kW). This phenomenon starts to notice after first hours of testing, becoming more important when 40 hours have elapsed. This is explained because the ground surrounding the borehole heat exchanger increases its temperature, as seen in the figures 5, 6 and 7, achieving a temperature gradient and activating the advective heat transfer mechanism. This is observed more clearly in layers composed by permeable materials such peat and gravel (around 10, 19 and 25 meters depth). In figures 8, 9 y 10 an inverse phenomenon is detected during the ground recovery process, decreasing the temperature more quickly at depths mentioned above.

From the analysis carried out is deduced that, in the thermal response tests performed under standard conditions in locations with a groundwater presence, the effective thermal conductivity value is overestimated, which influences in the ground heat exchanger dimensioning. This positive effect will not always occur during the operation of the ground source heat pump installation because, among the factors that activate it, one of them is a continuous injection thermal power that not represents the usual heat pump operation, characterized by short work cycles. For this reason, the proposed analysis model is considered interesting because allows the designers choose the effective thermal conductivity value to which is more suitable to calculate with, the one that best represents the thermal conductivity of the materials that make up the stratigraphic column of the borehole or the one that includes groundwater phenomena which helps heat transmission.

6. CONCLUSIONS

Detecting the effects of groundwater flow in the effective thermal conductivity is very difficult in standard thermal response test, obtaining a value which is not the thermal conductivity of the geological formation but a higher value. Existing models that consider convection required an extra resource effort with more complex data analysis, longer data collection periods or equipment to monitor more parameters.

In this work, a modification of finite and infinite line analysis models has been done in order to take into account the groundwater phenomenon in the thermal conductivity analysis. The implementation of this methodology has been possible thanks to an exhaustive thermal characterization of a borehole located at Universitat Politècnica of València, analysing the data of three different thermal powers injections during long periods of time in addition to a correct characterization of the ground undisturbed temperature and an analysis of the ground temperature behaviour before, during and after the injections. This analysis has allowed to identify the activation of the advective heat transfer mechanism explaining the increases detected in previous works in the value of the thermal conductivity depending on time and injected power. Using this background, a phenomenological parametrization of this groundwater effect in the thermal conductivity has been obtained introducing in the finite and infinite line source models an expression for the effective thermal conductivity that depends on a true thermal conductivity, the difference between the average fluid temperature and the undisturbed ground temperature and a parameter that quantifies the effect produced by underground water currents. The results show that it is possible to estimate the true thermal conductivity value regardless the power injected or the time elapsed in the test, fitting the values much better in the modified line source model than in the standard line source model.

So it can be concluded that, together with an adequate characterization of undisturbed ground temperature, which is already carried out in standard TRT, it is possible to analyse the effects of the groundwater flow without increase the TRT experimental measurements using the conventional analysis models, quantifying the “masking” of true thermal conductivity value due to groundwater flow action over time. Applying this methodology, GSHE designers can obtain the results of the geological effective thermal conductivity allowing a proper calculation without increase the cost of testing that benefits the development of GSHP installations.

ACKNOWLEDGEMENTS

This work has been supported by the Spanish Government under project “Modelado, simulación y validación experimental de la transferencia de calor en el entorno de la edificación” (ENE2008-00599/CON).

REFERENCES

[1] Spitler J.D., Bernier M. Advances in ground-source heat pump systems. Chapter 2 Vertical borehole ground heat exchanger design methods. Elsevier, 2016, http://dx.doi.org/10.1016/B978-0-08-100311-4.00002-9

[2] Aresti Lazaros, Christodoulides Paul, Florides Georgios. A review of the design aspects of ground heat exchangers. Renewable and Sustainable Energy Reviews 98, 2018, pp. 757 – 773

[3] Sanner B., Hellström G., Spitler J.D., Gehlin S. More than 15 years of mobile Thermal Response Test—A summary of experiences and prospects. In Proceedings of the European Geothermal Congress, Pisa, Italy, 3–7 June 2013

[4] Reuß M., Pröll Markus, Nordell Bo. IEA ECES -Annex 21 – Thermal Response Test. 2019

[5] ISO 17628:2015 Geotechnical investigation and testing — Geothermal testing — Determination of thermal conductivity of soil and rock using a borehole heat exchanger

[6] ASHRAE. HVAC Applications: Geothermal Energy. ASHRAE Handbook. American Society of Heating, Refrigerating and Air-Conditioning Engineers Inc., 2007, pp. 32.1-32.2

[7] IGSHPA. Closed-loop/geothermal heat pump systems: design and installation standards, 2013 edition. Oklahoma State University: International Ground Source Heat Pump Association, 2013

[8] Austin, W. A. Development of an in-situ system for measuring ground thermal properties. M.S. thesis, Oklahoma State University, Stillwater, OK, USA, 1998, 177 pp.

[9] Eklöf, F., Gehlin, S. A mobile equipment for Geothermal Response Test. M.S. thesis, Lulea University of Technology, Lulea, Sweden, 65 pp.

[10] Badenes B., Mateo Pla M. A., Lemus-Zúñiga L. G., Sáiz Mauleón B., Urchueguía J. F. On the influence of operational and control parameters in thermal response testing of borehole heat exchangers. Energies 2017, 10, 1328, doi:10.3390/en10091328

[11] Bandos T., Montero Á., Fernández de Córdoba P. and Urchueguía J.F. Improving parameter estimates obtained from thermal response tests: effect of ambient air temperature variations. Geothermics 42, 2011, pp. 136-143

[12] Spitler Jeffrey D., Gehlin Signhild E.A. Thermal response testing for ground source heat pump systems—An historical review. Renewable and Sustainable Energy Reviews 50, 2015, pp. 1125-1137

[13] Ingersoll L.R., P.H. Theory of the Ground Pipe Heat Source for the Heat Pump. ASHVE Transactions, Vol.54, 1948

[14] Mogensen P. Fluid to duct wall heat transfer in duct system heat storages. The international Conference on Subsurface Heat Storage in Theory and Practice, Appendix, Part II, Stockholm, 1983, pp. 652-657

[15] Hart D, Couvillion R. Earth coupled heat transfer. National Water Well Association, 1986

[16] Hellström G. Thermal analysis of duct storage system. Department of Mathematical Physics, University of Lund, Lund, Sweden, 1991, 262 pp.

[17] Witte H.J., Van Gelder G.J. y Spitler J.D. In Situ measurement of ground thermal conductivity: a Dutch perspective. ASHRAE Transactions 108, 2002, pp.1-10

[18] Eskilson P. Thermal Analysis of Heat Extraction Boreholes. Ph.D. Thesis, Lund University, Longde, Sweden, 1987

[19] Lamarche L., Beauchamp B. A new contribution to the finite line-source model for geothermal boreholes. Energy Build 39, 2007, pp. 188–198

[20] Bandos T.V., Montero Á., Fernández E., Santander J.L.G., Isidro J.M., Pérez J., Fernández de Córdoba P., Urchueguía, J.F. Finite line-source model for borehole heat exchangers: effect of vertical temperature variations. Geothermics 38, 2009, pp. 263–270

[21] Zeng H.Y., Diao N.R., Fang Z.H. A finite line-source model for boreholes in geothermal heat exchangers. Heat Transf Res 31, 2002, pp. 558–567, http://dx.doi.org/10.1002/htj. 10057

[22] Ingersoll L.R., Zobel O.J., Ingersoll A.C. Heat Conduction with Engineering, Geological, and Other Applications. Phys Today, 1955, pp. 8-17, http://dx.doi.org/10. 1063/1.3061951

[23] Carslaw H.S., Jaeger J.C. Conduction of heat in solids. 2nd ed Oxford: Clarendon Press, 1959

[24] Kavanaugh S. Simulation and experimental verification of vertical ground-coupled heat pump systems. Stillwater, 1985

[25] Bernier M.A. Ground-coupled heat pump system simulation. ASHRAE Trans 106, 2001, pp. 605–616

[26] Sanner B., Mands E., Sauer M. K., Grundmann E. Thermal response test, a routine method to determine thermal ground properties for GSHP design. 9th International IEA Heat Pump Conference, Zürich, Switzerland, 20 – 22 May, 2008

[27] Aresti L., Florides G.A., Christodoulides P. Computational modelling of a ground heat exchanger with groundwater flow. Bulg Chem Commun 48, 2016, pp. 55–63

[28] Gustafsson A.M., Westerlund L. Heat extraction thermal response test in groundwater-filled borehole heat exchanger—investigation of the borehole thermal resistance. Renewable Energy 36, 2011, pp. 2388–2394

[29] Spitler Jeffrey D., Javed Saqib, Ramstad Randi Kalskin. Natural convection in groundwater-filled boreholes used as ground heat exchangers. Applied Energy 164, 2016, pp. 352 – 365

[30] Sutton M.G., Nutter D.W., Couvillion, R.J. A ground resistance for vertical bore heat exchangers with groundwater flow. J. Energy Resour. Technol. 125, 2003, pp. 183–189

[31] Diao N., Li Q., Fang Z. Heat transfer in ground heat exchangers with groundwater advection. Int. J. Therm. Sci. 43 (12), 2004, pp. 1203–1211

[32] Molina-Giraldo N., Blum P., Zhu K., Bayer P., Fang Z. A moving finite line source model to simulate borehole heat exchangers with groundwater advection. Int. J. Therm. Sci. 50, 2011, pp. 2506–2513

[33] V. Wagner, P. Blum, M. Kübert, P. Bayer, Analytical approach for ground water influenced thermal response tests of grouted borehole heat exchangers, Geothermics 46, 2013, pp. 22–31

[34] Witte H.J., van Gelder A.J. Geothermal response tests using controlled multi-power level heating and cooling pulses (MPL– CP): Quantifying ground water effects on heat transport around a borehole heat exchanger. Proceedings Ecostock, Richard Stockton College of New Jersey, May 31–June 2, 2006

[35] Urchueguía J. F., Lemus Zúñiga L. G., Oliver Villanueva J. V., Badenes B., Mateo Pla M. A., Cuevas J. M. How reliable are standard thermal response tests? An assessment based on long-term thermal response tests under different operational conditions. Energies 2018, 11, 3347; doi:10.3390/en11123347

[36] Spitler J.D., Javed S. Advances in ground-source heat pump systems. Chapter 3 Calculation of borehole thermal resistance. Elsevier, 2016. http://dx.doi.org/10.1016/B978-0-08-100311-4.00003-0

[37] Witte, H.J. Error analysis of thermal response tests. Appl. Energy 109, 2013, pp. 302–311

[38] Luo J., Tuo J., Huang W., Zhu Y., Jiao Y., Xiang W., Rohn, J. Influence of groundwater levels on effective thermal conductivity of the ground and heat transfer rate of borehole heat exchangers. Appl. Therm. Eng. 128, 2018, pp. 508–516

[39] Beier R. A., Mitchell M. S., Spitler J. D., Javed S. Validation of borehole heat exchanger models against multi-flow rate thermal response tests. Geothermics 71, 2018, pp. 55 – 68

[40] Lamarche L., Raymond J., Koubikana Pambou C.H. Evaluation of the internal and borehole resistances during thermal response tests and impact on ground heat exchanger design. Energies 2018, 11, 38; doi:10.3390/en11010038

[41] Chiasson A.C., Rees S.J., Spitler J.D. A preliminary assessment of the effects of ground-water flow on closed-loop ground-source heat pump systems. ASHRAE Transactions 106(1), 2000, pp. 380-393

[42] Montero A., Urchueguía J.F., Martos J., Badenes B., Picard M.A. Ground temperature profile while thermal response testing. In Proceedings of the European Geothermal Congress 2013, Pisa, Italy, 3–7 June 2013, pp. 1–6

[43] Montero A., Urchueguía J.F., Martos J. Badenes, B. Ground temperature recovery time after BHE insertion In Proceedings of the European Geothermal Congress 2013, Pisa, Italy, 3–7 June 2013, pp. 1–6

[44] N. Aranzabal et al. Extraction of thermal characteristics of surrounding geological layers of a geothermal heat exchanger by 3D numerical simulations. Appl. Therm. Eng., 99, 2016, pp. 92–102

[45] Martos J., Montero Á., Torres J., Soret J., Martínez G. and García-Olcina R. Novel wireless sensor system for dynamic characterization of borehole heat exchangers. Sensors 11, 2011, pp. 7082-7094

[46] Magraner T., Montero Á., Quilis S. and Urchueguía J.F. Comparison between design and actual energy performance of a HVAC-ground coupled heat pump system in cooling and heating operation. Energy and Buildings 42, 2010, pp. 1394–1401